Bioorganic & Medicinal Chemistry 18 (2010) 5528–5534

Contents lists available at ScienceDirect

Bioorganic & Medicinal Chemistry

journal homepage: www.elsevier.com/locate/bmc

Conjugating folic acid to gold nanoparticles through glutathione for targeting and detecting cancer cells

Zhaowu Zhang, Jing Jia, Youqun Lai, Yanyan Ma, Jian Weng, Liping Sun *

Department of Biomaterials, College of Materials, Xiamen University, Xiamen 361005, People's Republic of China

ARTICLE INFO

Article history:
Received 13 April 2010
Revised 12 June 2010
Accepted 15 June 2010
Available online 19 June 2010

Keywords:
Gold nanoparticles
Glutathione
Folic acid
Folate receptor
Cancer cells

ABSTRACT

Gold nanoparticles (GNPs) were modified with glutathione (GSH) to form GSH-capped GNPs, which have carboxyl groups on the surface of these nanoparticles. Then folic acid (FA) was conjugated with GNPs through the reaction between amino group of FA and carboxyl group of GSH. These folic acid-conjugated nanoparticles (FA-GSH-GNPs) were stable in aqueous solution over a broad range of pH and ionic strength values. The targeting of FA-GSH-GNPs in human cervices carcinoma cells (HeLa cells) with high-level folate receptor expression was confirmed by transmission electron microscopy (TEM) and confocal laser scanning microscopy (CLSM). No cellular uptake of these nanoparticles was observed in A549 cells lack of folate receptor. HeLa cells and mouse fibroblasts incubated with FA-GSH-GNPs were assayed by measuring the relative absorbance of the supernatant collected at low-speed centrifugation. Based on this simple spectroscopic method, HeLa cells have been detected with a detection limit of 10^2 cells/mL.

1. Introduction

Gold nanoparticles (GNPs) play important roll in the biomedical fields for their advantages compared with other agents. They have strong surface-plasmon-enhanced absorption and scattering, which is important for imaging labels and contrast agents.[1–5] Moreover, GNPs are not susceptible to photobleaching and they appear biocompatible on human cells.[6] Another advantage is their facile bioconjugation and biomodification. The surface of GNPs has strong binding affinity towards thiols, disulfides, and amines.[7] In particular, the simple Au-thiol chemistry allows the surface conjugation with various peptides, proteins, and DNA, either via a naturally available thiol group such as cysteine or some others which have incorporated thiol group.[8,9]

Nanoparticles are usually uptaken into cells by three different pathways, which are fluid-phase endocytosis, phagocytosis, and receptor-mediated endocytosis, respectively.[10] Sometimes, the extent of internalization of metallic nanoparticles is severely limited by the low efficiency of uptake by endocytosis. Hence, in order to increase the internalization of nanoparticles, the nanoparticle surface is modified with a ligand known to be efficiently internalized by target cells via receptor-mediated endocytosis. Surface functionalized GNPs by conjugation with a specific antibody, for example, anti-epidermal growth factor receptor (EGFR) for epithelial cancer cells, have been developed for the application in the diagnosis and thermo-phototherapy of cancer cells.[11–14] Besides, many other agents, such as aptamer, peptides, antibodies and proteins have also been documented for cancer cell targeting.[15–21] The receptor for folic acid constitutes a useful target for tumor specific delivery, compared to the above different strategies for receptor-mediated endocytosis of nanoparticles, because folate receptors (FAR) are up-regulated on a variety of human cancers, including cancers of the breast, ovaries, endometrium, kidneys, colon, brain, and myeloid cells of hematopoietic origin.[22,23] The lack of folate receptors in nonproliferating normal cells differentiates them from tumor cells.[24] FA has a high affinity to cell surface receptors. Moreover, it is nonimmunogenic, highly stable, inexpensive and has small molecular size. Thus it facilitates the easy internalization of nanoparticles through cell membrane.[25] Therefore, the development of an efficient gold nanoparticles-folate conjugate system is a current challenge in this area. Numerous attempts using poly(a-midoamine) (PAMAM) dendrimers, poly(D,L-lactic-co-glycolic acid) (PLGA), poly(ethylene glycol) (PEG), PLL(poly-L-Lysine) and their block copolymers to develop biodegradable hydrophilic folate-nanoparticle conjugate for cancer targeting systems have been reported.[26–30] Though these targeting systems have good biocompatibility and internalization efficiency, the large size of these macromolecule-based systems does not facilitate intravenous delivery.[31] In order to effectively pass through the blood stream to reach the target cell of interest, the size of the nanoparticle–folate-conjugate system and its colloidal stability in the physiological environment should be taken into account. In this paper, a simple chemical method has been developed to couple folic acid on the gold nanoparticles' surface through glutathione (GSH). GSH is a small-sized natural tripeptide (γ-Glu-Cys-Gly) that

* Corresponding author. Tel./fax: +86 592 2183181.
E-mail address: sunliping@xmu.edu.cn (L. Sun).

0968-0896/$ - see front matter © 2010 Elsevier Ltd. All rights reserved.
doi:10.1016/j.bmc.2010.06.045

contains an -SH group, an amino group and two carboxyl groups. Moreover, it is the most abundant thiol species in the cytoplasm and the major reducing agent in biochemical processes.[32] We used it as a stabilizer and a coupling agent in synthesis of GSH-capped GNPs (GSH-GNPs). GSH was immobilized on the surface of gold nanoparticles via the thiol group from the cysteine moiety, and FA was conjugated with GNPs through the reaction between carboxyl group of GSH and amino group of FA. GSH also provided an amino group which could couple with fluorescein isothiocyanate (FITC) to form fluorescently labeled nanoparticles.[33] The targeting of FA-GSH-GNPs in HeLa cells with high-level folate receptor expression was confirmed by transmission electron microscopy and confocal laser scanning microscopy. Based on a simple spectroscopic method, HeLa cells have been detected with a detection limit of 10^2 cells/mL.

2. Results and discussion

2.1. Preparation of folic acid-functionalized gold nanoparticles

We improved the conventional method to synthesize GNPs by citrate reduction of $HAuCl_4$ under microwave.[34,35] As shown in Scheme 1, FA-GSH-GNPs were prepared by a three-step approach. The thiol group of glutathione can be easily attached to the surface of gold nanoparticles to form stable Au–S bond.[36–38] DCC and NHS are used to activate the carboxyl groups of GSH, forming a highly reactive intermediate (NHS-carboxylate). The activated carboxyl groups react subsequently with the free amino group presented in folic acid, resulting in the formation of folic acid-conjugated nanoparticles (FA-GSH-GNPs).

2.2. Characterization of folic acid-functionalized gold nanoparticles

The transmission electron micrograph of FA-GSH-GNPs indicates that the particles are uniformly dispersed with a significant narrow size range of 15–20 nm (Fig. 1A). The average particle size is 13 nm. UV–vis absorption spectra of GNPs and FA-GSH-GNPs are presented in Figure 1B. The unmodified nanoparticles display a characteristic surface plasmon absorption at 520 nm, while FA-conjugated GNPs show a surface plasmon band around 528 nm. This red-shift (8 nm) in the position of the maximum absorption indicates that FA has interacted with GNPs.

The hydrodynamic diameters and zeta potentials of GNPs, GSH-GNPs and FA-GSH-GNPs were measured at pH 7 to further verify the presence of folic acid on the nanoparticles. Table 1 shows that the hydrodynamic diameter of GNPs is smaller than GSH-GNPs and FA-GSH-GNPs. This phenomenon might be explained by two reasons: firstly, modification of GSH and FA onto the surface of GNPs increases the particle size; secondly, the amine and carboxyl groups of GSH and FA attract counterions from the solution to form electrical double layer. Therefore the increased double layer thickness results in a larger particle diameter.

The zeta potentials of GNPs dispersed in water are negatively charged because the nanoparticles are coated by citrate ion which possess three carboxyl groups (citric acid $pK_{a1} = 3.13$, $pK_{a2} = 4.76$, $pK_{a3} = 6.40$).[39] At pH 7, all the carboxyl groups are deprotonated. So GNP carries three net negative charge. After conjugation with GSH through Au–S bond, the citrate ions are replaced by GSH, which has a free amine group and two carboxyl groups. According to the dissociation constant of GSH ($pK_{a1} = 8.4$, $pK_{a2} = 5.0$, $pK_{a3} = 6.0$),[40] the amine group is protonated, while the two carboxyl groups are deprotonated at neutral pH. Since one carboxyl group is neutralized by the positive charge of amino group, GSH-GNP carries a net negative charge. For FA-modified GNP, only one carboxyl group of FA is deprotonated to form COO^- at pH 7 (FA $pK_{a1} = 2.3$, $pK_{a2} = 8.3$).[41] There are two FA molecules conjugated on the nanoparticles, but as one of the two deprotonated carboxyl groups is neutralized by the amino group of GSH, FA-GSH-GNP also carries a net negative charge. The change in the amount of surface charge alters the dielectric state of the nanoparticles, consequently resulting in decrease of the zeta potential values. FA-GSH-GNPs and GSH-GNPs confer a less negative zeta potential values compared with GNPs because they carry one net charge while GNP carries three net charges.

Adding HCl, NaOH, or NaCl to the FA-GSH-GNPs aqueous solution did not markedly affect the UV–Vis spectra in a NaCl concentration range of 0.01–0.5 mol/L (Fig. 2A) and a pH range of 3–11

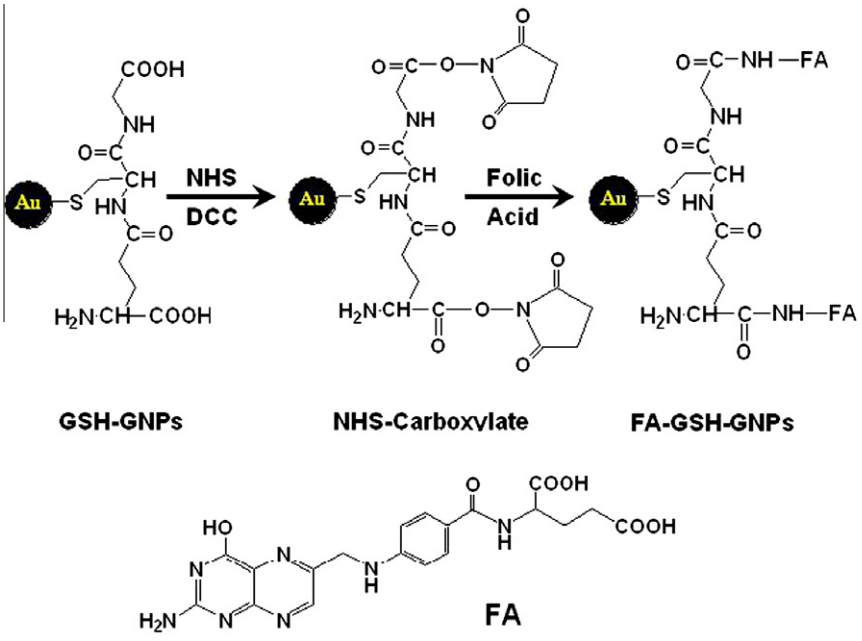

Scheme 1. The preparation of folic acid-functionalized gold nanoparticles.

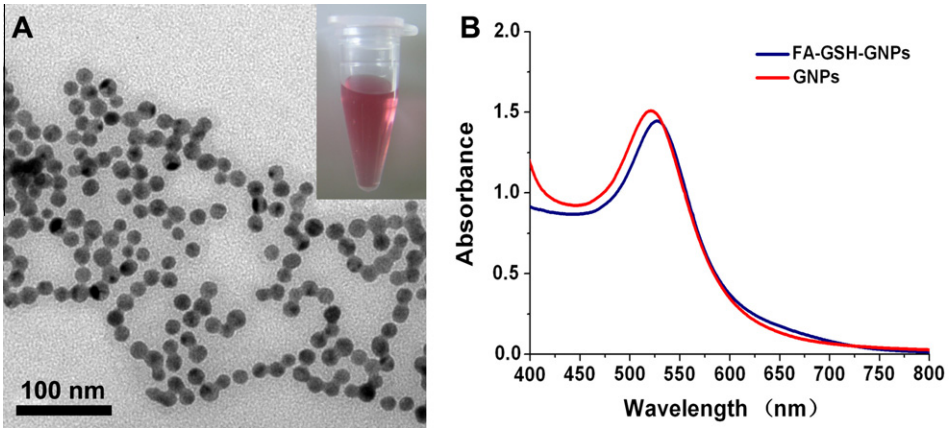

Figure 1. TEM image of FA-GSH-GNPs (A) and UV–vis spectra of GNPs and FA-GSH-GNPs (B).

Table 1
Hydrodynamic diameter and zeta potential of GNPs, GSH-GNPs and FA-GSH-GNPs at pH 7

Nanoparticles	GNPs	GSH-GNPs	FA-GSH-GNPs
Hydrodynamic diameter (nm)	27.5 ± 3.6	30 ± 4.5	36.4 ± 4.2
Zeta potential (mV)	−29.05 ± 1.4	−22.35 ± 2.1	−15.7 ± 1.8

(Fig. 2B). These results indicate that the FA-GSH functionalized gold nanoparticles have good stability.

Figure 3 showed that the surface composition of GNPs significantly changed after GSH and FA modification. The peaks at binding energy of 80–90, 160–170, 280–290, 395–405, 528–538 eV are ascribed to Au 4f, S 2p, C 1s, N 1s and O 1s electros, respectively (Fig. 3A).[42] The detection of nitrogen in the sample confirmed the attachment of GSH and FA on the surface of GNPs. XPS spectra clearly showed two peaks at 84.0 and 87.5 eV (Fig. 3B), which correspond to the Au $4f_{7/2}$ and Au $4f_{5/2}$ peak, respectively.[43] The peak for S 2p was fitted into two peaks at 162.2 eV and 163.7 eV (Fig. 3C). The peak at 162.2 eV indicates the formation of Au–S bond between GSH and gold nanoparticles.[44] N 1s was fitted into two peaks at 398.85 and 400.6 eV, corresponding to $-NH_2$ and –NHCO (Fig. 3D).[30]

2.3. Determination of glutathione and folic acid content

According to the result of elemental analyses, the content of S in FA-GSH-GNPs is 0.702×10^{-5} mol, which reflects the same amount of GSH bound onto the nanoparticle surface. The amount of FA coupled on the nanoparticles was evaluated by measuring the absorbance of the product at 358 nm (FA $\varepsilon = 15{,}760\ M^{-1}\ cm^{-1}$).[45] It was found that 1.498×10^{-5} mol FA were linked to the nanoparticles. As the GSH–FA ratio (0.702×10^{-5}:1.498×10^{-5}) is close to 1:2, about two FA molecules are estimated to bind to one GSH-GNP.

2.4. Cytotoxicity assay

The cytotoxicity of FA-GSH-GNPs to HeLa and mouse fibroblast (FB) cells was analyzed by MTT assay. Cells cultured with FA-GSH-GNPs have similar proliferation compared with the untreated cells ($p > 0.5$) (Fig. 4). When the concentration of FA-GSH-GNPs reached 100 μg/mL, the cell survival rates of HeLa and FB cells were 93.3% and 97.6%, respectively. These results reveal that FA-GSH-GNPs have good biocompatibility.

2.5. In vitro cellular uptake study

The conjugation of FITC to FA-GSH-GNPs enabled confocal microscopic imaging of the cellular uptake. As shown in Figure 5A, HeLa cells treated with FA-GSH-GNPs display fluorescence signals, which was associated with the specific uptake of these nanoparticles into the cytoplasm. In contrast, A549, a human lung adenocarcinoma epithelial cell line which lacks folate receptors,[46] showed very weak fluorescence signals in Figure 5B. This observation suggests that the binding and intracellular uptake did not occur in the cells expressing low folate receptor levels.

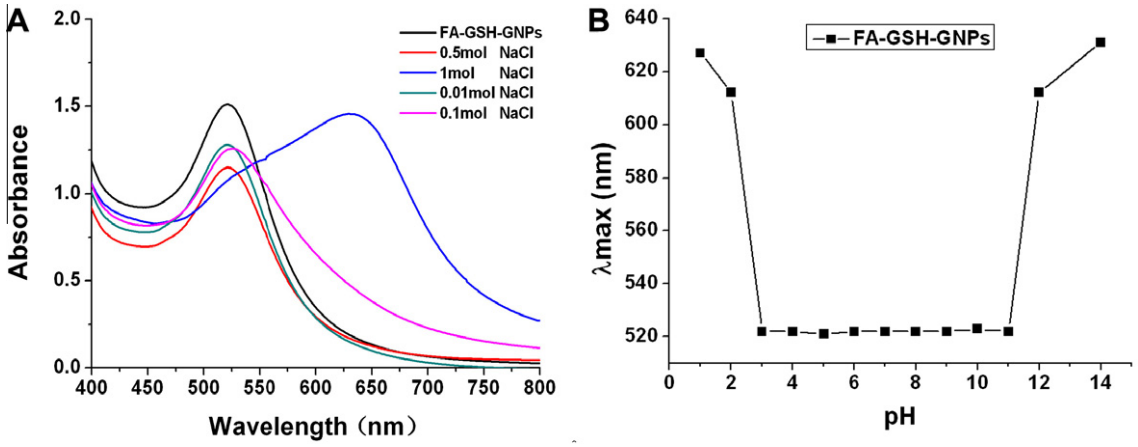

Figure 2. (A) The stability of FA-GSH-GNPs in NaCl solution at different concentration (0.01–1 mol/L), (B) the stability of FA-GSH-GNPs at different pH (1.0–14.0).

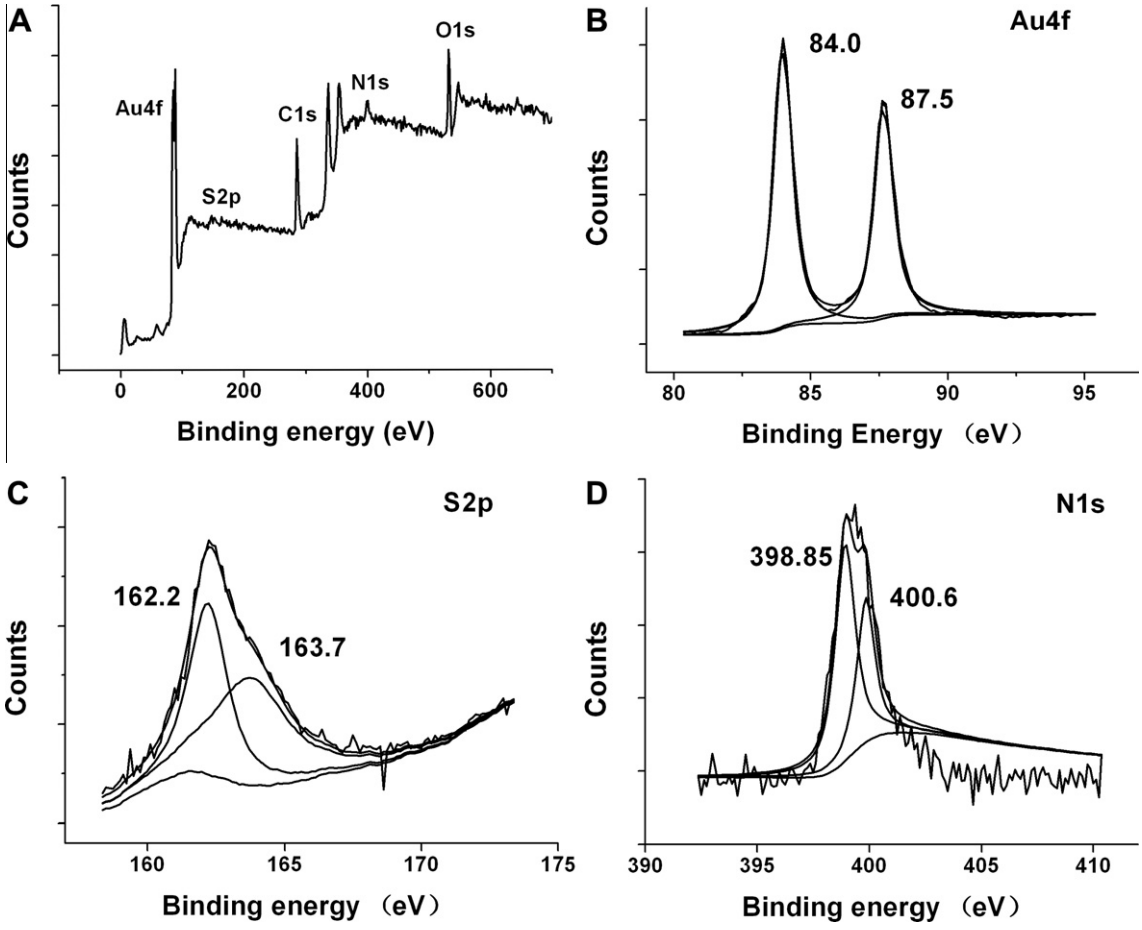

Figure 3. The XPS of FA-GSH-GNPs presenting (A) a survey, (B) Au 4f, (C) S 2p, (D) N 1s spectra.

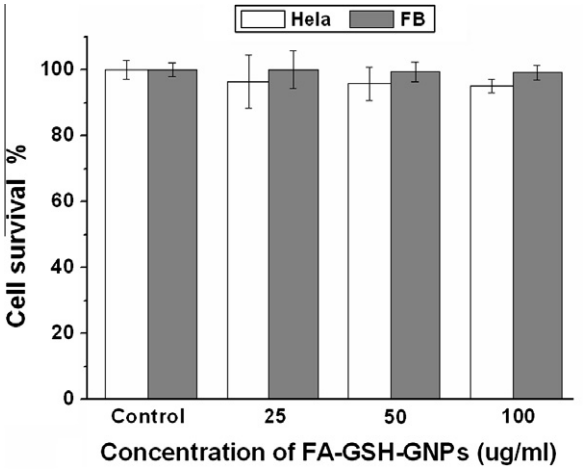

Figure 4. Effects of FA-GSH-GNPs on the viability of HeLa and FB cells. No nanoparticles were added to the control groups. The cells were treated with FA-GSH-GNPs for 24 h at concentrations of 25, 50 and 100 μg/mL.

In order to further confirm the distribution of FA-GSH-GNPs in cancer cells, TEM image was done. For HeLa cells treated with FA-GSH-GNPs, the nanoparticles were clearly visible as higher-contrast regions inside the cytoplasm (Fig. 6A). In contrast, A549 cells lack of folate receptors revealed no uptake of the nanoparticles after exhaustive TEM observation (Fig. 6B). The TEM studies confirmed the high specificity of FA-GSH-GNPs for targeting HeLa cells with high-level folate receptor expression, and corroborated the confocal imaging data. FA-GSH-GNPs are taken up by HeLa cells through folate receptor-mediated endocytosis and trapped in endosomes. These endosomes then fuse with lysosomes for processing before being transported to the cell periphery for excretion.[47,48]

2.6. Cancer cell assay

In this study, FA-GSH-GNPs were successfully used to detect cancer cells. HeLa cells were taken as target cells while FB cells lack of folate receptors were used as control cells. The nanoparticles cannot be removed by low-speed centrifugation (1000 rpm). But when they bind to the HeLa cells through folate receptor, they can be easily deposited together with the cells at 1000 rpm, leading to decrease in absorbance of the supernatant at 528 nm, which is called relative absorbance (ΔA) in this paper. ΔA indirectly represents the amount of nanoparticles which bind to target cells. In order to determine the limit of detection for the assay, ΔA at 528 nm was recorded for each amount of cells and plotted in Figure 7. It is obvious that the higher the HeLa cell concentration, the higher the ΔA is, suggesting that more nanoparticles are being deposited at 1000 rpm by targeting HeLa cells. ΔA of the control cells (FB) has nearly no change in comparable to the blank because FA-GSH-GNPs cannot bind to fibroblast cells lack of folate receptors, the nanoparticles still remain in the supernatant after low-speed centrifugation. This assay showed a linear correlation between ΔA (A) and the concentration of HeLa cells (C) ranging from 10^2 to 10^5 cells/mL ($A = 1.0465 + 0.0857$ C, correlation coefficient of

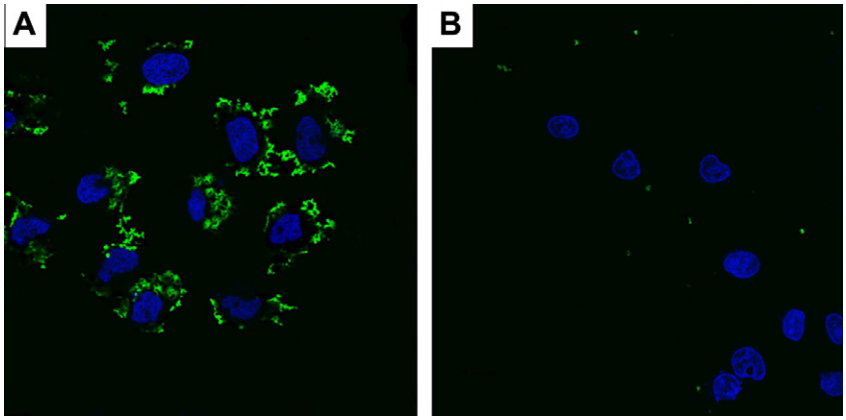

Figure 5. Nanoparticle uptake visualized by confocal microscopy. Images were acquired at 600× magnification. The cells were incubated with FITC-labeled FA-GSH-GNPs for 2 h.

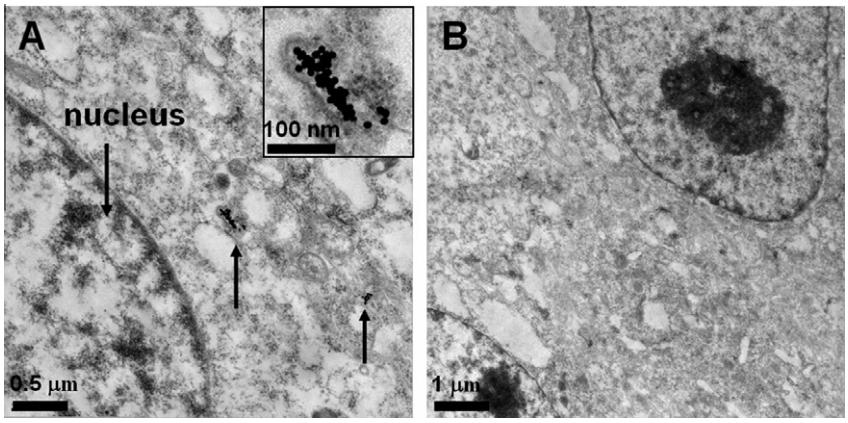

Figure 6. TEM micrographs of HeLa cells (A) and A549 cells (B) incubated with FA-GSH-GNPs for 2 h.

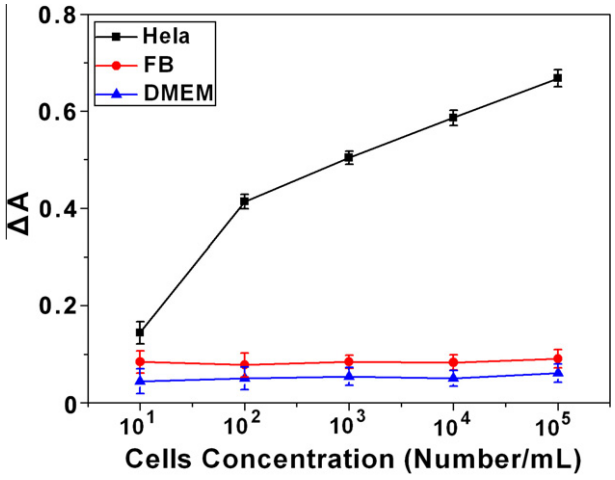

Figure 7. ΔA of the target HeLa cells (black) and fibroblasts (red). The blank sample contains no cell (culture medium with nanoparticles, blue).

0.9984). At low cell concentration (10^1 cells/mL), there is no significant difference of ΔA at 528 nm between cancer cells and control cells ($p > 0.05$). In the range of 10^2–10^5 cells/mL, HeLa cells and FB can be distinguished clearly by a significant difference of ΔA of all four groups ($p < 0.05$). This detection limit (10^2 cells/mL^{-1}) was close to that of 90 cells (namely 3×10^2 cells/mL^{-1}) using aptamer-conjugated gold nanoparticles for cancer cells detection.[15] Based on these results, the assay has demonstrated excellent sensitivity and selectivity.

3. Conclusions

In summary, a simple process has been developed to synthesize folic acid-conjugated gold nanoparticles by using glutathione as coupling agent. FA-GSH-GNPs were water-soluble, stable, and had good biocompatibility. Combined confocal microscopy and TEM analyses showed that these nanoparticles could successfully target tumor cells overexpressing the folate receptors. FA-GSH-GNPs have been demonstrated for the sensitive and selective detection of human HeLa cells through utilizing the unique spectral properties of gold nanoparticles and the excellent selectivity of folic acid. In addition, since the surface of the GSH-GNPs could be similarly functionalized with other targeting ligands besides folic acid, they should serve as an effective carrier for targeted drug delivery to different types of cancer. FA-GSH-GNPs might have potential in cancer diagnosis and therapy.

4. Experimental

4.1. Reagents and apparatus

$HAuCl_4$, sodium tris-citrate, dimethyl sulphoxide (DMSO) were purchased from Xilong Chemical (Guangdong, China). Folic acid (FA), glutathione (GSH), dicyclohexyl carbodiimide (DCC), *N*-hydroxysuccinimide (NHS) were obtained from Shanghai

Sangon Biological and Engineering Company (Shanghai, China). FITC, 4,6-diamidino-2-phenylindole (DAPI), 3-(4,5-dimethyl-thiazol-2-yl)-2,5-diphenyl-tetrazolium bromide (MTT), trypsin, penicillin and streptomycin were from Sigma–Aldrich Chemicals (Scotland, UK). Dulbecco Modified Eagle's Medium (DMEM), DMEM with no phenol red, RPMI 1640 medium and fetal bovine serum (FBS) were purchased from Gibco BRL/Life Technologies (Paisley, UK). All reagents were of analytical grade. Milli-Q water (18.2 MΩ) was used in all of the experimental processes.

All UV–vis spectra were collected on a Beckman H800 UV–vis spectrophotometer with 1 nm resolution. The determinations of zeta potential and hydrodynamic size of the nanoparticles were carried out using Zetasizer Nano-ZS (Malvern Instruments Ltd, UK). Each data point for zeta potential is an average of at least 15 measurements at pH 7. The morphology of particles were characterized by TEM-JEM-2100 HC, JEOL, Japan) operated at an accelerating voltage of 120 kV. The fluorescence intensity was measured at 530 nm in a Perkin Elmer LS-55 fluorescence spectrophotometer. The surface composition of FA-GSH-GNPs was analyzed in an PHI Quantum 2000 Scanning ESCA Microprobe (PHI, America) using Al Kα excitation source. Elemental analyses were performed by Elementar Vario EL III (Elementar Analysensysteme GmbH, Germany).

4.2. Preparation of folic acid-functionalized gold nanoparticles

Gold nanoparticles were prepared basically as we did before.[34,35] All the used glasswares in the following procedures were cleaned in a bath of freshly prepared aqua regia, rinsed thoroughly in ultrapure water and dried in cabinet drier. GNPs solution (10 mL) was deaerated by pure nitrogen (>99%). Then, 50 μL of 0.05 mol GSH solution was added into the solution. The resulting solution was stirred for 12 h for reaction, and then was dialyzed for another 6 h to remove the extra free small molecules. 25 μL of DCC solution (0.05 mol/L in dimethyl sulfoxide (DMSO)) and the same amount of NHS solution (0.05 mol/L in DMSO) were added into the above dialyzed solution, the mixture was stirred for 1 h and folic acid was added into the solution, which was stirred over-night and then dialyzed for 12 h to remove the vestigial molecules. FA functionalized gold nanoparticles (FA-GSH-GNPs) were thus obtained in this solution. The stability of FA-GSH-GNPs in different concentrations of NaCl solution (0.01–1 mol/L) and at different pH values (1–14) were measured by UV–vis spectrometry. The pH of aqueous solutions was adjusted by adding 1 M HCl or 1 M NaOH.

Fluorescently labeled nanoparticles were prepared by the following procedures: FITC (0.1 mol/L) was added to FA-GSH-GNPs solution in the dark, then incubated at room temperature on an orbital plate shaker for 24 h, and dialyzed until the fluorescence intensity of the solution did not decrease.

4.3. Determination of glutathione and folic acid content

The amount of folic acid in the conjugate was evaluated by measuring the absorbance of the product at 358 nm (folic acid $\varepsilon = 15{,}760\ M^{-1}\ cm^{-1}$).[45] Using elemental analyzer (Elementar Vario EL III) measurements, we have determined the amount of S in FA-GSH-GNPs.

4.4. In vitro cellular studies

4.4.1. Cell culture

The cells cultivated for in vitro experiments were mouse fibroblast L929, HeLa and A549. HeLa cells, a human cervices carcinoma cell line that is known to overexpress folate receptors, and L929 cells were cultured in Dulbecco Modified Eagle's Medium (DMEM). A549 cells, a human lung adenocarcinoma epithelial cell line, were grown in RPMI 1640 medium. All media were supplemented with 10% heat-inactivated fetal bovine serum (FBS) and 1% penicillin–streptomycin at 37 °C in a 5% CO_2 and 95% air humidified atmosphere.

4.4.2. Cytotoxicity assay

HeLa or L929 cells were added to each well of 96-well tissue culture plate at a density of 5×10^5 cells/mL and incubated for 18 h. Then 20 μL of FA-GSH-GNPs nanoparticles were added to each well at different concentrations (25, 50 and 100 μg/mL), incubated for 24 h at 37 °C. No nanoparticles were added to the control cells. Discard the culture medium and then wash the plate with PBS. Add 180 μL of culture medium and 20 μL of MTT (5 μg/mL) to each well and incubated for 4 h at 37 °C. Remove the culture medium, wash the plate with PBS and subsequently add 200 μL of DMSO to each well. The culture plate was incubated for 30 min at 37 °C. OD values at a wavelength of 490 nm were measured with a microplate reader (Bio-Rad Laboratories, USA).

4.4.3. Cellular uptake study

HeLa cells were incubated over-night in 6-well plate at a density of 5×10^5 cells/mL. After confluence was achieved, 500 μL of FITC-labeled FA-GSH-GNPs was added to each well. After 2 h of incubation, all wells were washed three times with PBS, fixed with 5% formaldehyde in PBS, and nuclei were stained for 5 min with 100 μL DAPI (0.1 mg/mL). The staining solution was removed by washing three times with PBS. The images were taken by a confocal laser scanning microscope (Leica TCS SP5, Germany). All confocal images were taken immediately after incubation and washing steps.

HeLa and A549 cells were incubated with FA-GSH-GNPs for 2 h, washed three times with PBS and fixed with 2.5% glutaraldehyde for 4 h. The cells were then post-fixed in 1% osmium tetraoxide for 2 h, dehydrated in graded concentrations of ethanol (25%, 50%, 70%, 80%, 90%, 95%, and 100%) and washed in propylene oxide. Cell samples were then embedded in Epon (Canemco Inc., Quebec, Canada) and thin-sectioned. Thin sections of 60–70 μm were collected on copper grids and stained with a 1:1 mixture of methanol and lead citrate. The grids were visualized using a JEM-2100 TEM.

4.5. Cancer cell assay

HeLa and L929 cells (FB) cells were analysed. For each assay, 300 μL of FA-GSH-GNPs (10 nmol) were added to 100 μL of DMEM culture medium (no phenol red) with different concentrations of cells (10^1, 10^2, 10^3, 10^4 and 10^5/mL), then incubated for 30 min at 4 °C in a 500 μL microcentrifuge tube (Beckman), and centrifuged at 1000 rpm for 5 min. The supernatant was withdrawn and the absorbance was measured. Culture medium with no cells but containing the same amount of nanoparticles was taken as the blank. ΔAbsorbance (ΔA) was calculated according to the following formula: $\Delta A = A_0 - A_1$ (A_0 = absorbance of blank, A_1 = absorbance of supernatant). The absorbance values were obtained with the Beckman H800 UV–vis spectrophotometer at 528 nm. Each experiment was repeated at least five times.

4.6. Statistical analysis

Data were presented as means ± SE from at least three independent experiments and analyzed by Student's *t*-test. Differences at $p < 0.05$ were considered statistically significant.

Acknowledgments

This research has been supported by the National Natural Science Foundation of China (30900350) and the Open Fund of State

Key Laboratory for Physical Chemistry of Solid Surfaces, Xiamen University (200602).

References and notes

1. Hainfeld, J. F.; Slatkin, D. N.; Focella, T. M.; Smilowitz, M. H. *Br. J. Radiol.* **2006**, *79*, 248.
2. Huang, X.; El-Sayed, I. H.; Quan, W.; El-Sayed, M. A. *J. Am. Chem. Soc.* **2006**, *128*, 2115.
3. Mukherjee, P.; Bhattacharya, R.; Wang, P.; Wang, L.; Basu, S.; Nagy, J. A. *Clin. Cancer Res.* **2005**, *11*, 3530.
4. Hirsch, L. R.; Stafford, R. J.; Bankson, J. A.; Sershen, S. R.; Rivera, B.; Price, R. E. *PNAS* **2003**, *100*, 13549.
5. Prashant, K. J.; El-Sayed, I. H.; El-Sayed, M. A. *Nanotoday* **2007**, *2*(1), 18.
6. Connor, E. E.; Mwamuka, J.; Gole, A.; Murphy, C. J.; Wyatt, M. D. *Small* **2005**, *1*(3), 325.
7. Katz, E.; Willner, I. *Angew. Chem., Int. Ed.* **2004**, *43*, 6042.
8. Naka, K.; Itoh, H.; Tampo, Y.; Chujo, Y. *Langmuir* **2003**, *19*, 5546.
9. Lee, J. S.; Ulmann, P. A.; Han, M. S.; Mirkin, C. A. *Nano Lett.* **2008**, *8*(2), 529.
10. Yang, P. H.; Sun, X. J.; Chiu, F.; Sun, H.; He, Q. Y. *Bioconjugate Chem.* **2005**, *16*, 494.
11. Sokolov, K.; Follen, M.; Aaron, J.; Pavlova, I.; Malpica, A.; Lotan, R.; Kortum, R. R. *Cancer Res.* **2003**, *63*, 1999.
12. Tsai, S. W.; Liaw, J. W.; Hsu, F. Y.; Chen, Y. Y.; Lyu, M. J.; Yeh, M. H. *Sensors* **2008**, *8*, 6660.
13. He, H.; Xie, C.; Ren, J. *Anal. Chem.* **2008**, *80*, 5951.
14. Yang, J.; Eom, K.; Lim, E. K.; Park, J.; Kang, Y. D.; Yoon, S.; Na, S.; Koh, E. K.; Suh, J. S.; Huh, Y. M.; Kwon, T. Y.; Haam, S. *Langmuir* **2008**, *24*, 12112.
15. Medley, C. D.; Smith, J. E.; Tang, Z.; Wu, Y.; Bamrungsap, S.; Tan, W. *Anal. Chem.* **2008**, *80*, 1067.
16. Pan, C.; Guo, M.; Nie, Z.; Xiao, X.; Yao, S. *Electroanalysis* **2009**, *21*(11), 1321.
17. Pujals, S.; Bastus, N. G.; Pereiro, E.; Lopez-Iglesias, C.; Puntes, V. F.; Kogan, M. J.; Giralt, E. *ChemBioChem* **2009**, *10*, 1025.
18. El-Sayed, I. H.; Huang, X.; El-Sayed, M. A. *Nano Lett.* **2005**, *5*(5), 829.
19. Patra, H. K.; Banerjee, S.; Chaudhuri, U.; Lahiri, P. A.; Dasgupta, K. *Nanomedicine* **2007**, *3*, 111.
20. Li, J.; Wang, L.; Liu, X.; Zhang, Z.; Guo, H.; Liu, W.; Tang, S. *Cancer Lett.* **2009**, *274*, 319.
21. Nativo, P.; Prior, I. A.; Brust, M. *ACS Nano* **2008**, *2*(8), 1639.
22. Gabizon, A.; Horowitz, T.; Goren, D.; Tzemach, D.; Mandelbaum, F. S.; Qazen, M. M.; Zalipsky, S. *Bioconjugate Chem.* **1999**, *10*, 289.
23. Sudimack, J.; Lee, R. J. *Adv. Drug Deliv. Rev.* **2000**, *41*, 147.
24. Xu, L.; Pirollo, K. F.; Chang, E. H. *J. Controlled Release* **2001**, *74*, 115.
25. Sega, E. I.; Low, P. S. *Cancer Metastasis Rev.* **2008**, *27*, 655.
26. Shi, X.; Wang, S.; Meshinchi, S.; Antwerp, M. E.; Bi, X.; Lee, I.; Baker, J. R. *Small* **2007**, *3*(7), 1245.
27. Dixit, V.; Bossche, J. V.; Sherman, D. M.; Thompson, D. H.; Andres, R. P. *Bioconjugate Chem.* **2006**, *17*, 603.
28. Kim, S. H.; Jeong, J. H.; Joe, C. O.; Park, T. G. *J. Controlled Release* **2005**, *103*, 625.
29. Sonvico, F.; Mornet, S.; Vasseur, S.; Dubernet, C.; Jaillard, D.; Degrouard, J.; Hoebeke, J.; Duguet, E.; Colombo, P.; Couvreur, P. *Bioconjugate Chem.* **2005**, *16*, 1181.
30. Mohapatra, S.; Mallick, S. K.; Maiti, T. K.; Ghosh, S. K.; Pramanik, P. *Nanotechnology* **2007**, *18*, 385102.
31. Kohler, N.; Sun, C.; Wang, J.; Jhang, M. *Langmuir* **2005**, *21*, 8858.
32. Lim, I. S.; Mott, D.; Njoki, P. N.; Pan, Y.; Zhou, S. Q.; Zhong, C. J. *Langmuir* **2008**, *24*, 8857.
33. Qaqish, R. B.; Amiji, M. M. *Carbohydr. Polym.* **1999**, *38*, 99.
34. Liu, F. K.; Chang, Y. C.; Ko, F. H.; Chu, T. C. *Mater. Lett.* **2004**, *58*, 373.
35. Sun, L.; Zhang, Z.; Wang, S.; Zhang, J.; Li, H.; Ren, L.; Weng, J.; Zhang, Q. *Nanoscale Res. Lett.* **2009**, *4*, 216.
36. Liu, L.; Zhu, X.; Zhang, D.; Huang, J.; Li, G. *Electrochem. Commun.* **2007**, *9*, 2547.
37. Chen, W.; Tu, X.; Guo, X. *Chem. Commun.* **2009**, *17*, 36.
38. Hong, R.; Han, G.; Fernandez, J. M.; Kim, B. N.; Forbes, S.; Rotello, V. M. *J. Am. Chem. Soc.* **2006**, *128*, 1078.
39. Gulicovski, J. J.; Erovi, L. S.; Milonji, S. K.; Popovic, I. G. *J. Serb. Chem. Soc.* **2008**, *73*, 825.
40. Aemas, M. T.; Mederos, A.; Gili, P.; Dominguez, S.; Molina, R. H.; Lorenzo, P.; Baran, E. J.; Araujo, M. L.; Brito, F. *Polyhedron* **2001**, *20*, 799.
41. Akhtar, M. J.; Khan, M. A.; Ahmad, I. *J. Pharma. Biomed.* **1999**, *25*, 269.
42. Moulder, J. F.; Stickle, W. F.; Sobol, P. E.; Bomben, K. D. *Handbook of X-ray Photoelectron Spectroscopy*; Perkin-Elmer: Minnesota, 1992.
43. Zhao, W.; Gonzaga, F.; Li, Y.; Brook, M. A. *Adv. Mater.* **2007**, *19*, 1766.
44. Bourg, M. C.; Badia, A.; Lennox, R. B. *J. Phys. Chem. B* **2000**, *104*, 6562.
45. Barbara, S.; Arpicco, S.; Peracchia, M. T.; Desmaele, D.; Hoebeke, J.; Renoir, M.; Dangelo, J.; Cattel, L.; Couvreur, P. *J. Pharm. Sci.* **2000**, *89*, 1452.
46. Bharali, D. J.; Lucey, D. W.; Jayakumar, H.; Pudavar, H. E.; Prasad, P. N. *J. Am. Chem. Soc.* **2005**, *127*, 11364.
47. Bhattacharya, R.; Patra, C. R.; Earl, A.; Wang, S.; Katarya, A.; Lu, L.; Kizhakkedathu, J. N.; Yaszemski, M. J.; Greipp, P. R.; Mukhopadhyay, D.; Mukherjee, P. *Nanomedicine* **2007**, *3*, 224.
48. Chithrani, B. D.; Stewart, J.; Allen, C.; Jaffray, D. A. *Nanomedicine* **2009**, *5*, 118.